

Journal of Materials Chemistry A

Accepted Manuscript



This is an *Accepted Manuscript*, which has been through the Royal Society of Chemistry peer review process and has been accepted for publication.

Accepted Manuscripts are published online shortly after acceptance, before technical editing, formatting and proof reading. Using this free service, authors can make their results available to the community, in citable form, before we publish the edited article. We will replace this *Accepted Manuscript* with the edited and formatted *Advance Article* as soon as it is available.

You can find more information about *Accepted Manuscripts* in the [Information for Authors](#).

Please note that technical editing may introduce minor changes to the text and/or graphics, which may alter content. The journal's standard [Terms & Conditions](#) and the [Ethical guidelines](#) still apply. In no event shall the Royal Society of Chemistry be held responsible for any errors or omissions in this *Accepted Manuscript* or any consequences arising from the use of any information it contains.

Cite this: DOI: 10.1039/x0xx00000x

Received 00th January 2012,
Accepted 00th January 2012

DOI: 10.1039/x0xx00000x

www.rsc.org/

Stabilizing Amorphous V₂O₅/Carbon Nanotube Paper Electrode with Conformal TiO₂ Coating by Atomic Layer Deposition for Lithium Ion Batteries

Ming Xie,^{a,b} Xiang Sun,^c Hongtao Sun,^c Tim Porcelli,^b Steven M. George,^{b,d} Yun Zhou^{*.e} and Jie Lian^{*.c}

Amorphous V₂O₅ (a-V₂O₅) thin films were conformally coated onto the surface of hydroxyl (–OH) functionalized multi-walled carbon nanotubes (CNTs) and carbon nanotube (CNT) paper using atomic layer deposition (ALD). In order to achieve 3 Li⁺ intercalation (442mAh/g) and prevent V₂O₅ dissolution at 1.5V, a conformal TiO₂ protective layer is coated on surface of V₂O₅/CNT. Free-standing paper electrode can be made by vacuum filtration or coating pre-fabricated CNT paper directly. The electrochemical characteristics of the TiO₂/V₂O₅/CNT paper electrode were then determined using cyclic voltammetry and galvanostatic charge/discharge curves. Because the TiO₂ and V₂O₅ ALD films were ultrathin, the poor electrical conductivity and low ionic diffusivity of V₂O₅ did not limit the ability of the V₂O₅ ALD films to display high specific capacity and high rate capability. High discharge capacity of ~400mAh/g is obtained for 15 cycle ALD TiO₂ coated 50 cycle ALD V₂O₅/CNT samples by depositing pre-fabricated CNT paper. We believe this is the highest capacity for V₂O₅ cathodes reported in literatures. The capacities for the a-V₂O₅/CNT nanocomposites are higher than the bulk theoretical values. The extra capacity is attributed to additional interfacial charge storage resulting from the high surface area of the a-V₂O₅/CNT nanocomposites. These results demonstrate that metal oxide ALD on high surface-area conducting carbon substrates can be used to fabricate high power and high capacity electrode materials for lithium ion batteries. In addition, ultrathin and conformal TiO₂ ALD coating can be used to mitigate the dissolution and capacity fading of the cathode.

Introduction

Lithium-ion batteries (LIBs) are one of the most promising energy storage technologies resulting from their high energy density and reasonable rate capability.^{1, 2} LIBs have received significant attention for applications in portable electronics. Additional improvements in energy density, lifetime stability and rate capability are needed for the further implementation of LIBs in electric

vehicles. These improvements may be provided by new materials and architectures for LIBs.^{3, 4}

Vanadium pentoxide, V₂O₅, was first reported as an intercalation cathode material for LIBs by Whittingham in 1975.⁵ Since then, extensive studies have been made due to its high capacity, high output voltage, and low cost.⁶⁻⁸ However, the intrinsic low-diffusion coefficient of lithium ions (10^{-12} cm² s⁻¹)⁹ and poor

electronic conductivity (10^{-2} to 10^{-3} S cm^{-1})¹⁰ in crystalline V_2O_5 hinder the practical application of this material. So far, V_2O_5 cathode has only been commercialized by Panasonic for small electronics. One of its derivatives, $\text{Ag}_2\text{V}_4\text{O}_{11}$ has been used for power source in medical devices,^{11,12} where Ag increases the electronic conductivity during discharge. Further improvements on its rate capability and lifetime are needed for application in EVs. In 2007, Subaru released G4E electric car which used V_2O_5 as cathode with a pre-lithiated anode. It claimed that the energy density of this type battery is almost 2-3 times higher than manganese-based LIBs. In 2010, DBM Energy equipped an Audi A2 electric vehicle with its new V_2O_5 -Li metal polymer battery and set a long distance record of 603 kilometres (375 miles) travelled on a single charge.

However, some major problems hinder V_2O_5 -based LIBs from the further development. Several phase transitions of $\text{Li}_x\text{V}_2\text{O}_5$ can occur depending on the amount of lithium insertion, namely α (for $x < 0.01$), ϵ ($0.35 < x < 0.7$), and δ (for $x = 1.0$) phases, respectively.^{13, 14} When $x \leq 1$, the phase transitions are fully reversible.¹⁵ Therefore, V_2O_5 usually has three voltage plateaus. However, when more lithiums are inserted ($x > 1$), a structural reconstruction leads to a partially irreversible transformation from δ -phase to γ -phase.¹³ This γ -phase can only be reversibly cycled in the stoichiometric range $0 < x < 2$ without changing the γ -type structure.¹³ With further lithiation (up to $x = 3$), the γ -phase will irreversibly transform to the ω -phase with a rock-salt type structure. Therefore, it is usually to limit the discharge voltage of V_2O_5 to 2V to prevent unwanted structure changes and lifetime decay.^{16,17} However, if V_2O_5 can be reversibly discharged to 1.5V, the theoretical capacity of 442mAh/g can be achieved with the maximum amount of 3Li^+ intercalation.^{16, 18} In addition, crystalline V_2O_5 suffers poor cycle life since its crystal structure can be damaged by prolonged charge/discharge cycles. Three voltage plateaus of crystalline V_2O_5 usually disappear after extensive cycling due to amorphization. Crystal deformation associated with lithiation may be relaxed in small crystallites with a high surface area that also leads to higher ionic conductivity. Therefore, nanocrystalline or amorphous V_2O_5 (a- V_2O_5) is a promising alternative cathode material.¹⁹⁻²²

The problems of low ionic diffusion and electrical conductivity with V_2O_5 can be addressed by depositing ultrathin a- V_2O_5 films on high surface area and high electrical conductivity carbon substrates. The a- V_2O_5 films can be deposited using atomic layer deposition

(ALD). ALD is based on sequential self-limiting reactions and provides precise control in film uniformity, thickness, composition and morphology.²³ ALD can deposit thin films on high aspect ratio substrates.^{24, 25} ALD also yields strong chemical bonding between the substrate and the deposited film that can enhance the cycle stability of the film during energy storage applications.

ALD has recently been successfully used to deposit metal oxides on carbon substrates for a variety of electrochemical applications. The metal oxide ALD films can enhance the capacity stability of carbon anodes in LIBs.^{26, 27} The metal oxide ALD coatings can also serve as active Li^+ storage materials on carbon supports for LIBs.^{17, 28, 29} Metal oxide films on carbon substrates can also serve to increase charge storage for supercapacitor applications.³⁰⁻³²

However, a- V_2O_5 also faces several issues. The first problem is the dissolution of electrode in the electrolyte, especially for nanostructured and poor crystallized materials whose surface area is often much larger than bulk and well crystallized materials.⁸ The second one is related with the poor mechanical strength of amorphous electrodes.³³ Therefore, and it may lose contact between particles,³⁴ especially during the repeated lithium-ion insertion/extraction process.

ALD nanocoatings, particularly Al_2O_3 , have been shown to enhance the capacity stability of anodes and cathodes for lithium ion batteries (LIBs) in our earlier work.³⁵⁻³⁷ Metal oxides coating can modify the electrode surface chemistry and increase the mechanical strength of electrodes.³⁸⁻⁴¹ However, conformal Al_2O_3 ALD film adds an insulating layer between the electrolyte and electrode. The thickness has to be carefully controlled in order to achieve the balance between lithium ion diffusion and prevention of vanadium dissolution. Compared to Al_2O_3 , TiO_2 polymorphs, including anatase, rutile, and $\text{TiO}_2(\text{B})$, have also been extensively studied as anodes for LIBs.⁴²⁻⁴⁸ TiO_2 delivers a high discharge voltage plateau of ~ 1.7 V and has a small volume expansion of $\sim 4\%$ during lithiation/delithiation.^{49, 50} TiO_2 has also been used as a protective coating on electrodes.⁵¹⁻⁵⁵

In this paper, we deposited a- V_2O_5 cathode film by ALD directly onto carbon nanotube powders and carbon nanotube (CNT) paper for LIBs. In order to improve the cycling performance of V_2O_5 at an extended voltage window (down to 1.5V), we deposited conformal amorphous TiO_2 as a protective layer by ALD. Two different electrode fabrication sequences are compared. Deposition

of V₂O₅ directly onto CNT paper show higher capacity and better rate capability. A much improved cycling performance is achieved with 15 cycles TiO₂ ALD coating, while maintaining an excellent rate capability.

Experimental Details

A. Materials Synthesis

V₂O₅ ALD films were grown on hydroxyl terminated CNT powders or CNT paper using a rotary ALD reactor.^{56, 57} The rotary reactor agitates the powders during ALD and prevents particle aggregation. V₂O₅ ALD was deposited utilizing vanadyl oxytriisopropoxide (VOTP) and H₂O as precursors. For the V₂O₅ ALD, VOTP and HPLC (high performance liquid chromatography) grade H₂O were both obtained from Sigma-Aldrich. The VOTP ALD reaction sequence was: i) dose VOTP to 1.0 Torr for 120 seconds; ii) evacuate reaction products and excess VOTP; iii) dose N₂ to 20.0 Torr for 60 seconds and then evacuate N₂ (repeat 5 times); iv) dose H₂O to 1.0 Torr for 120 seconds; v) evacuate reaction products and excess H₂O; vi) dose N₂ to 20.0 Torr for 60 seconds and then evacuate N₂ (repeat 5 times). This sequence constitutes one cycle of V₂O₅ ALD. The V₂O₅ ALD was performed at 150°C. Using this reaction sequence, the V₂O₅ film thickness was precisely controlled by the number of V₂O₅ ALD reaction cycles.

V₂O₅ ALD on pristine CNTs will have initial nucleation difficulties due to the lack of reactive sites as reported previously.⁵⁶ V₂O₅ ALD is expected to nucleate and grow only at defects and step edges on CNTs in the absence of an adhesion layer. Growth at these defects will result in a distribution of V₂O₅ nanoparticles. Hydroxyl terminated multiwalled CNTs were purchased from Nanostructured & Amorphous Materials, Inc. CNT paper was purchased from Inorganic Specialists Inc. Hydroxyl groups on CNTs help form conformal V₂O₅ film.

TiO₂ ALD was deposited using utilizing titanium tetrachloride (TiCl₄) and H₂O as precursors according to the following surface reactions:⁵⁸



The performance of both of these A and B reactions constitutes one TiO₂ ALD cycle. For the TiO₂ ALD, TiCl₄ (99.8%, Strem

Chemicals) and high performance liquid chromatography (HPLC) grade H₂O were obtained from Sigma-Aldrich.

The TiO₂ ALD reactions were performed using static exposures in the rotary ALD reactor. The reaction sequence was: i) dose TiCl₄ to 1.0 Torr for 120 seconds; ii) evacuate the reaction products and excess TiCl₄; iii) dose N₂ to 20.0 Torr for 60 seconds and then evacuate N₂ (repeat 5 times); iv) dose H₂O to 1.0 Torr for 120 seconds; v) evacuate the reaction products and excess H₂O; vi) dose N₂ to 20.0 Torr for 60 seconds and then evacuate N₂ (repeat 5 times). The TiO₂ ALD was performed at 120°C.

B. Fabrication of Free-Standing V₂O₅/CNT Paper Electrode

The free-standing electrodes can be made by two different methods. V₂O₅ and TiO₂ with desired ALD cycle number are deposited onto -OH terminated CNT powders or pre-fabricated CNT paper sequentially. The coated CNT powders are then mixed with 10% uncoated CNTs by mass. Free-standing electrode was then fabricated using a filtration method using a proprietary solvent developed by Inorganic Specialists Inc. Briefly, 90% V₂O₅/CNT nanocomposites and 10% pristine CNT powders by mass were dispersed in the solvent without surfactants. No organic binder was needed. The diameter of the filter paper was 47 mm. The whole process is called Method 1 in this paper. Method 2 coats pre-fabricated CNT paper directly. After deposition, the coated CNT paper is used for characterization without further treatment. The areal V₂O₅ mass loading for both methods is 2-3 mg/cm².

C. Materials Characterization

The phase, crystallinity and microstructure of the V₂O₅/CNT were characterized by XRD using PAN analytical x-ray diffraction system and scanning electron microscopy by a Carl Zeiss Ultra 1540 Dual Beam FIB/SEM System, respectively. Thermogravimetric analysis (TGA) was performed in air from 20 °C to 800 °C at a heating rate of 10 °C/min in a TA Instrument TGA-Q50. Transmission electron microscopy (TEM) images were obtained using a JEOL JEM-2010 instrument with an operating voltage at 200 kV.

D. Electrochemical Measurements

All of the cells were assembled in an argon-filled dry box with paper electrode as cathode and Li metal as the reference electrode. The CNT-V₂O₅ was put directly against the stainless steel cap of

coin cell. A Celgard separator 2340 and 1 M LiPF₆ electrolyte solution in 1:1 w/w ethylene carbonate and diethyl carbonate (Novolyte) were used to fabricate the coin cells. Cyclic voltammetry (CV) measurement was carried out using a potentiostat VersaSTAT 4 (Princeton Applied Research) at a scan rate of 0.5 mV s⁻¹. Galvanostatic charge/discharge cycles were performed at a voltage range of 4-1.5 V using an Arbin BT 2000 testing station. 1C=440mA/g. Electrochemical impedance spectroscopy (EIS) were measured at a frequency range between 0.1 Hz-100 kHz and 10 mV amplitude with a coin cell configuration. The Nyquist plots were modelled by an equivalent circuit model. R_e is the electrolyte resistance, and CPE1 and R_s are the capacitance and resistance of the surface film formed on the electrodes, respectively. CPE2 and R_{ct} are the double layer capacitance and charge-transfer resistance, respectively, Z_w is the Warburg impedance.

Results and Discussion

An illustration of ultrathin TiO₂/V₂O₅ ALD films on CNTs by two different fabrication consequences, called Method 1 and Method 2, respectively, is displayed in Figure 1. Method 1 starts with OH-CNT powder, followed by V₂O₅ ALD deposition. V₂O₅/CNT powder are then mixed with 10% CNT to form a free-standing paper electrode by vacuum filtration. At the end, TiO₂ ALD is performed on V₂O₅/CNT paper electrode as a protective coating. Method 2 starts with pre-fabricated CNT paper, followed by V₂O₅ and TiO₂ ALD, sequentially. Paper electrode has many advantages: (1) the total weight of the electrodes is greatly reduced, since no binder, conductive additive, and current collector are needed; (2) the conductivity of the electrodes is greatly enhanced due to the good conductivity of the CNTs compared with the traditional carbon black. The sheet resistance of our samples is in the range of 3-7Ω/□; (3) the porous electrode structure facilitates electrolyte diffusion; (4) both of paper electrodes have excellent flexibility as shown in figure 1(c). In addition, ultrathin film thicknesses can greatly shorten both the Li⁺ ion diffusion length and electron transfer path to assure exceptional rate capability for the TiO₂/V₂O₅/CNT nanocomposite.

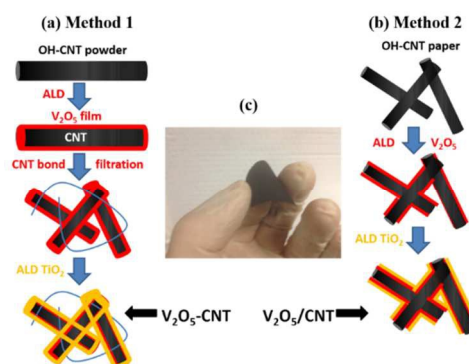


Figure 1. The procedure for preparing TiO₂/V₂O₅/CNT paper electrode by Method 1(a) and Method 2(b). (c) Paper electrode shows excellent flexibility.

Figure 2(a) shows a conformal coating of 20cycle TiO₂/50cycle V₂O₅ on CNT. No agglomerated particles can be seen after deposition, indicating that TiO₂ and V₂O₅ thin films are conformably coated on the surface of CNTs. This is a unique advantage for ALD over wet-chemistry based synthesis by which particle agglomeration is usually observed. In addition, the width along CNT is very uniform at ~29-30nm after deposition. Figure 2(b) shows the wall of the CNT after being coated with 20cycle TiO₂/50cycle V₂O₅ ALD. A very uniform and conformal composite film is observed with a total thickness of ~12 nm. There are no gaps or voids in the films or at the interfaces. This thin composite film should not affect the electron transport and ion diffusion. Electron conductivity through these films should be high resulting from electron tunnelling.⁵⁹ The thickness of the CNT coated with 20cycle TiO₂/50cycle V₂O₅ is larger than the thickness predicted by the growth rates for V₂O₅ ALD and TiO₂ ALD on flat substrates. The growth rate of V₂O₅ ALD on flat substrates is 0.8 Å/cycle at 150°C.⁶⁰ The growth rate of TiO₂ ALD on flat substrates is 0.6 Å/cycle at 120°C.⁶¹ However, earlier studies have reported ALD growth rates on high surface area powders of ~2 times the ALD growth rates on flat substrates.^{57, 62} These larger growth rates are believed to be caused in part by insufficient H₂O purging and the contribution of some chemical vapor deposition (CVD) to the ALD growth.^{57, 62} X-ray diffraction (XRD) patterns in supporting information Figure 1S show that 50 ALD cycle V₂O₅/CNT only have a broad graphene diffraction feature with 2θ at 24 degree.⁶³ No diffraction peaks from crystalline V₂O₅ are observed, indicating the amorphous nature of the as-deposited V₂O₅. EDS in Figure S2 confirms the existence of V and Ti, and elemental mapping in Figure S3 illustrates that they are uniformly deposited within each CNT agglomeration.

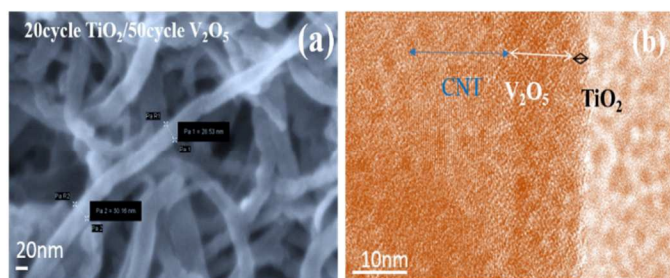


Figure 2. SEM and TEM of 20 cycle TiO_2 /50 cycle V_2O_5 on CNT

Figure 3 shows the TGA results that were used to obtain the V_2O_5 and TiO_2 mass loading on the CNT sample. Large weight losses were observed at the oxidation temperatures of $\sim 450^\circ\text{C}$ for the CNT sample. The weight percentage of the TiO_2 protective layer was obtained from the weight difference of the samples before and after the TiO_2 ALD coating. The mass percentage of the V_2O_5 ALD together with the TiO_2 protective layer was determined from the weight after annealing to 750°C in the TGA experiments. Based on the mass of the TiO_2 protective layer from the weight difference and the combined V_2O_5 ALD and TiO_2 ALD weight % from the TGA measurements, the mass loading of V_2O_5 is calculated to be 59 wt% for 50 V_2O_5 /CNT sample. The mass loading of V_2O_5 was also calculated to be 52 wt% and 12 wt% for the TiO_2 / V_2O_5 /CNT samples, respectively. These calculations assume that the carbon is completely removed following annealing to 750°C . This assumption is reasonable because there was negligible change in sample weights at temperatures above 600°C in additional TGA experiments.

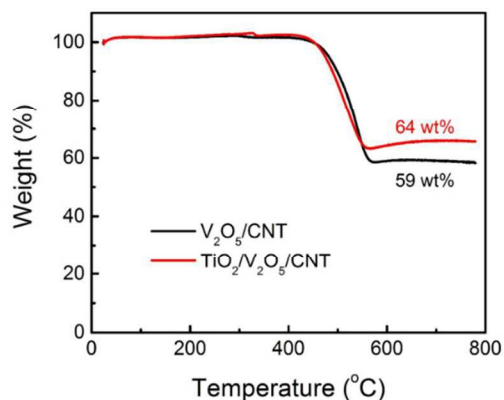


Figure 3. TGA of ALD TiO_2 / V_2O_5 /CNT composites.

Cyclic voltammograms (CV) of TiO_2 / V_2O_5 /CNT nanocomposites are measured between 1.5 and 4 V at a scan rate of 0.5 mV/s. The CV scan of a 15 cycle TiO_2 /50 cycle V_2O_5 /CNT nanocomposite is displayed in Figure 4(a). European convention is employed where voltage is more positive with scanning to the right and the anodic current is positive. The anodic current is expected to result from lithium extraction from V_2O_5 . As lithium ions are inserted into the layers of crystalline V_2O_5 , the phase transformation occurs consecutively from α - V_2O_5 to ϵ - $\text{Li}_{0.5}\text{V}_2\text{O}_5$ (3.35 V), δ - LiV_2O_5 (3.15 V), γ - $\text{Li}_2\text{V}_2\text{O}_5$ (2.26 V), and ω - $\text{Li}_3\text{V}_2\text{O}_5$ (1.87 V).^{15, 16} Among the various phases of $\text{Li}_x\text{V}_2\text{O}_5$, δ - LiV_2O_5 can be restored to pristine V_2O_5 through lithium deintercalation, while γ - $\text{Li}_2\text{V}_2\text{O}_5$ and ω - $\text{Li}_3\text{V}_2\text{O}_5$ (rock-salt type structure) are formed irreversibly.¹³ In the following anodic scanning, two peaks should be observed at around 2.67 and 3.26 V vs. Li/Li^+ , respectively, corresponding to the lithium extraction processes.^{19, 20} However, for our samples, both the anodic and cathodic current densities versus potential are very broad. No anodic or cathodic peaks are observed between 1.5–4 V that are commonly observed for crystalline V_2O_5 .^{16, 64–69} The featureless current density versus potential is consistent with amorphous V_2O_5 .⁷⁰ The featureless CV is consistent with the lack of crystalline phases during lithiation/delithiation and is due to the contribution from the amorphous phase. Amorphous V_2O_5 displays more “box-like” current versus voltage that is suggestive of capacitive behavior.

The voltage profile shown in Figure 4(b) is in a good agreement with CV curve. The voltage profiles show that the voltage decreases and increases progressively versus capacity during lithiation and delithiation, respectively. This progressive decrease and increase of the voltage during lithiation and delithiation is expected for amorphous V_2O_5 .⁷⁰ The voltage profiles for CNT and ALD TiO_2 on CNT are included in supporting information. Both of them have the slope behaviour. The initial discharge and charge capacity is 374mAh/g, and 390mAh/g, respectively. From the second cycle, both discharge/charge capacities reach ~ 397 mAh/g reversibly, corresponding to coulombic efficiency at nearly 100%.

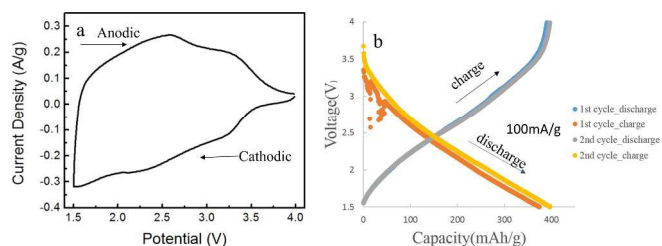


Figure 4. (a) CV curves of ALD TiO₂/V₂O₅/CNT paper electrode (b) Voltage profile of TiO₂/V₂O₅/CNT paper electrode.

Figure 5 shows the lifetime study and rate performance at various current densities in the extended voltage range between 1.5-4.0V. The contribution from CNT paper without any deposition is measured as 20mAh/g in this voltage window. It is well-known that the defects and edge plane in CNT structure significantly contribute to the lithium storage capacity.⁷¹ However, those sites preferably attract ALD precursors as compared to the graphene basal plane which is very inert to ALD precursors. Therefore, the capacity contribution from those defects and edge planes of CNT is limited after covered with V₂O₅ and TiO₂. In our previous study, we deposited 5 ALD cycles of Al₂O₃ (~0.5nm) on reduced graphene oxide powders.⁷² The thin Al₂O₃ film mimics the deposited material at the defects and edge planes of graphene, in that only intercalation between graphene layers can contribute to the capacitance of this composite. The capacity is only 258mAh/g, much lower than the covered graphene which usually has a capacity above 400mAh/g. Therefore, we believe that the actual capacity of CNT in here should be even lower than 20mAh/g measured without V₂O₅ and TiO₂ deposition from 4-1.5V.

The specific capacity of TiO₂/V₂O₅ is calculated based on the total weight obtained from TGA results. The long term cyclic stability is evaluated at a current density of 100 mA/g for 50 ALD cycles V₂O₅ with different ALD cycles of TiO₂. For samples made by method 1, the reversible capacity of 50 ALD cycles V₂O₅/CNT without TiO₂ coating continuously decays from 1st to the 100th cycle, and exhibits a capacitance less than 150 mAh/g after 100 cycles as shown in Fig. 5(a). In comparison, the 5, 10 and 15 ALD cycle TiO₂ coating on V₂O₅/CNT samples all exhibit much improved cycling stability. With the increase of the ALD cycle number, 20 cycle TiO₂ showed the best stability and its discharge capacity maintains at 300mAh/g after 100 cycles. In addition, TiO₂ does not jeopardize the rate capability of V₂O₅/CNT samples shown in Figure 5(b). When the current density increases from 0.23C to 2.3C, 74% of its capacity at 0.23C is still preserved, indicating an excellent rate capability. For

samples made by method 2, even higher discharge capacity of ~400mAh/g is obtained for 15 cycle TiO₂ coated V₂O₅/CNT samples. In addition to its protective role, TiO₂ can also contribute pseudocapacitance. We have studied pseudocapacitance of ALD TiO₂ thoroughly in our previous work.⁷³⁻⁷⁶ From 3-1.5V, TiO₂ has a capacity of ~75mAh/g as shown in SI. We can calculate the capacity of V₂O₅ by deducting the contribution from TiO₂ and CNT. The capacity of V₂O₅ is 461mAh/g. We also notice that V₂O₅/CNT without TiO₂ coating exhibit an exceptional discharge capacity of ~480mAh/g for the first several cycles, higher than the theoretical value of 442mAh/g. Higher capacities than theoretical predictions have been previously attributed to interfacial charge storage phenomena.^{42, 77-80} A similar explanation can be employed to explain the high capacity with excellent rate capacity in the current study on a-V₂O₅ ALD films on CNTs. In addition, the “box-like” appearance of the cathodic and anodic current densities is also consistent with capacitive interfacial charge storage behavior.^{81, 82} Charge storage in the electric double layer and on the V₂O₅ surface via Faradaic reactions can provide much higher capacities than the capacities in the V₂O₅ bulk alone. As a matter of fact, ALD V₂O₅ on CNT was studied as pseudocapacitive materials, exhibiting a very high capacity of 1550F/g.⁸³ 84% of its capacity at 0.23C is still preserved when the rate ramps to 2.3C. Higher capacity and better rate retention for samples prepared by method 2 is probably due to better electrical contact between CNTs. Method 2 deposits V₂O₅ onto a pre-fabricated CNT paper, thus taking advantage of high electrical inter-connection between CNTs. In method 1, all of CNTs are uniformly coated by ~12nm TiO₂/V₂O₅ films. Therefore, the resistance of electrodes will be much larger than samples prepared by Method 2. The same observation is found when ALD Al₂O₃ is coated on electrodes instead on electrode powders.^{35, 37}

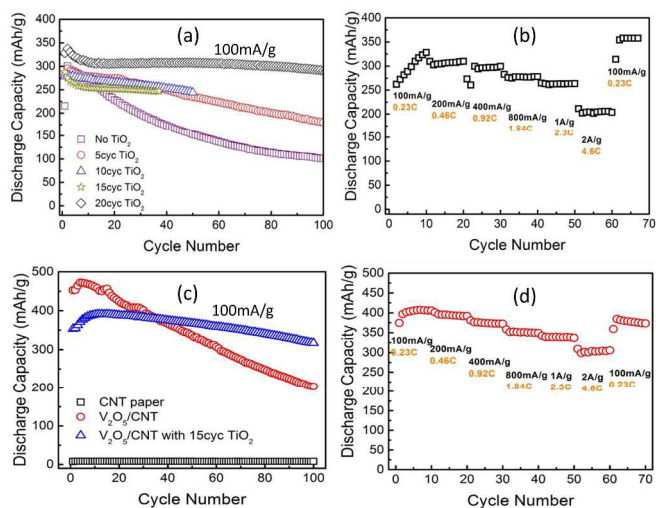


Figure 5. (a) Cycling performance of uncoated V_2O_5/CNT and V_2O_5/CNT with different TiO_2 thickness prepared by Method 1; (b) Rate performance of $TiO_2/V_2O_5/CNT$ prepared by Method 1; (c) Cycling performance of uncoated V_2O_5/CNT and V_2O_5/CNT with different TiO_2 thickness prepared by Method 2; (d) Rate performance of $TiO_2/V_2O_5/CNT$ prepared by Method 2.

We further examined V_2O_5/CNT with and without TiO_2 coating after 100 cycles at $100mA/g$ by electrochemical impedance spectroscopy (EIS) analysis. As shown in Figure 6, the charge transfer resistance with TiO_2 coating is much smaller than without TiO_2 coating after cycling, indicating the much more stable electrode structure and thinner interfacial layer between electrode and electrolyte. In addition, the migration of transition metals from the dissolution of cathode materials to anodes is well known for the increase of the impedance.⁸⁴⁻⁸⁶ TiO_2 coating prevents V dissolution from the cathode, therefore, much smaller impedance increase is observed compare to without TiO_2 coating.

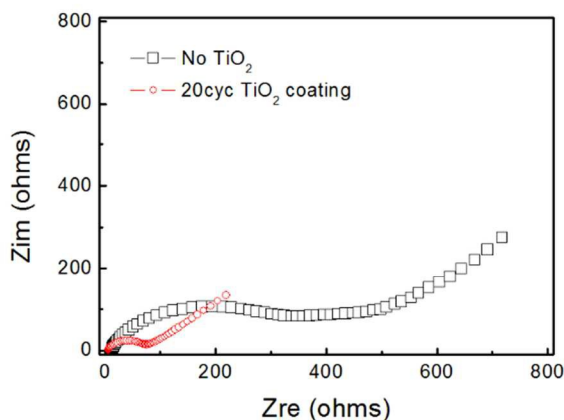


Figure 6. Nyquist plot of V_2O_5/CNT with and without TiO_2 after 100 cycles at $100mA/g$.

Conclusion

In summary, a- V_2O_5 has been synthesized on CNT by ALD and studied as cathode materials for lithium ion battery. TiO_2 as a protective coating is applied onto the surface of V_2O_5 by ALD as well. Coating on CNT paper directly gives higher capacity and better rate retention than on CNT powder. 15cycle $TiO_2/50$ cycle V_2O_5/CNT paper electrode delivers the discharge capacity of 400 mAh g^{-1} at $100mA/g$, approaching to the theoretical value of V_2O_5 . The dissolution problem of vanadium which is a major hurdle that limits V_2O_5 for cathode applications has been fully addressed by TiO_2 ALD coating, without sacrificing capacity and rate capability. We expect that the success of addressing the dissolution problem of vanadium will benefit the study of this material for other applications, such as aqueous lithium ion battery anodes and catalysis.

Acknowledgments

The work at Chongqing Normal University was supported by the Natural Science Foundation of China (No. 21301199), Chongqing Municipal Education Commission (KJ130601) and Chongqing Science and Technology Commission (cstc2014jcyjA50035). This work at Rensselaer Polytechnic Institute was supported by a NSF Career Award under the Award of DMR 1151028. This work at Wuhan ATMK Super EnerG Technologies Inc. is supported by the 3551 Recruitment Program of Global Experts by Wuhan East Lake Hi-Tech Development Zone, China. The work at the University of Colorado was supported by the Defense Advanced Research Project Agency (DARPA).

Notes and references

^a Wuhan ATMK Super EnerG Technologies, Inc., #7-5 JiaYuan Road, Wuhan, 430073, China

^b Department of Chemistry and Biochemistry, University of Colorado at Boulder, Boulder, Colorado 80309, USA.

^c Department of Mechanical, Aerospace & Nuclear Engineering, Rensselaer Polytechnic Institute, 110 8th Street Troy, NY 12180, USA.

^d Department of Mechanical Engineering, University of Colorado, Boulder, Colorado 80309, United States

^e Chongqing Normal University, College of Chemistry, Chongqing, 401311, China;

Corresponding author: yunzhou@cqnu.edu.cn (Yun Zhou)
lianj@rpi.edu (Jie Lian)

Electronic Supplementary Information (ESI) available: [details of any supplementary information available should be included here]. See DOI: 10.1039/b000000x/

1. J. M. Tarascon and M. Armand, *Nature*, 2001, 414, 359-367.
2. M. S. Whittingham, *Chem. Rev.*, 2004, 104, 4271-4301.
3. P. G. Bruce, B. Scrosati and J.-M. Tarascon, *Angew. Chem. Int. Edit.*, 2008, 47, 2930-2946.
4. G. Jeong, Y.-U. Kim, H. Kim, Y.-J. Kim and H.-J. Sohn, *Energy Environ. Sci.*, 2011, 4, 1986-2002.
5. M. S. Whittingham, *J Electrochem Soc*, 1975, 122, 713-714.
6. E. A. Ponzio, T. M. Benedetti and R. M. Torresi, *Electrochim Acta*, 2007, 52, 4419-4427.
7. Y. Wang, K. Takahashi, K. Lee and G. Z. Cao, *Adv Funct Mater*, 2006, 16, 1133-1144.
8. Y. Wang and G. Z. Cao, *Adv Mater*, 2008, 20, 2251-2269.
9. T. Watanabe, Y. Ikeda, T. Ono, M. Hibino, M. Hosoda, K. Sakai and T. Kudo, *Solid State Ionics*, 2002, 151, 313-320.
10. J. Muster, G. T. Kim, V. Krstic, J. G. Park, Y. W. Park, S. Roth and M. Burghard, *Adv Mater*, 2000, 12, 420-+.
11. A. Crespi, C. Schmidt, J. Norton, K. M. Chen and P. Skarstad, *J Electrochem Soc*, 2001, 148, A30-A37.
12. E. S. Takeuchi and W. C. Thiebolt, *J Electrochem Soc*, 1988, 135, 2691-2694.
13. J. M. Cocciantelli, J. P. Doumerc, M. Pouchard, M. Broussely and J. Labat, *J Power Sources*, 1991, 34, 103-111.
14. J. Galy, *J Solid State Chem*, 1992, 100, 229-245.
15. R. J. Cava, A. Santoro, D. W. Murphy, S. M. Zahurak, R. M. Fleming, P. Marsh and R. S. Roth, *J Solid State Chem*, 1986, 65, 63-71.
16. S. H. Ng, T. J. Patey, R. Buechel, F. Krumeich, J. Z. Wang, H. K. Liu, S. E. Pratsinis and P. Novak, *Phys Chem Chem Phys*, 2009, 11, 3748-3755.
17. X. Y. Chen, H. L. Zhu, Y. C. Chen, Y. Y. Shang, A. Y. Cao, L. B. Hu and G. W. Rubloff, *ACS Nano*, 2012, 6, 7948-7955.
18. A. Tranchant, R. Messina and J. Perichon, *J Electroanal Chem*, 1980, 113, 225-232.
19. S. H. Ng, S. Y. Chew, J. Wang, D. Wexler, Y. Tournayre, K. Konstantinov and H. K. Liu, *J Power Sources*, 2007, 174, 1032-1035.
20. M. Koltypin, V. Pol, A. Gedanken and D. Aurbach, *J Electrochem Soc*, 2007, 154, A605-A613.
21. J. M. McGraw, J. D. Perkins, J. G. Zhang, P. Liu, P. A. Parilla, J. Turner, D. L. Schulz, C. J. Curtis and D. S. Ginley, *Solid State Ionics*, 1998, 113, 407-413.
22. S. Passerini, J. J. Ressler, D. B. Le, B. B. Owens and W. H. Smyrl, *Electrochim Acta*, 1999, 44, 2209-2217.
23. S. M. George, *Chem. Rev.*, 2010, 110, 111-131.
24. J. W. Elam, D. Routkevitch, P. P. Mardilovich and S. M. George, *Chem. Mater.*, 2003, 15, 3507-3517.
25. R. G. Gordon, D. Hausmann, E. Kim and J. Shepard, *Chem Vapor Depos*, 2003, 9, 73-78.
26. Y. S. Jung, A. S. Cavanagh, L. A. Riley, S. H. Kang, A. C. Dillon, M. D. Groner, S. M. George and S. H. Lee, *Adv. Mater.*, 2010, 22, 2172-+.
27. I. Lahiri, S.-M. Oh, J. Y. Hwang, C. Kang, M. Choi, H. Jeon, R. Banerjee, Y.-K. Sun and W. Choi, *J. Mater. Chem.*, 2011, 21, 13621-13626.

28. C. M. Ban, M. Xie, X. Sun, J. J. Travis, G. K. Wang, H. T. Sun, A. C. Dillon, J. Lian and S. M. George, *Nanotechnology*, 2013, 24, 424002.
29. X. F. Li, X. B. Meng, J. Liu, D. S. Geng, Y. Zhang, M. N. Banis, Y. L. Li, J. L. Yang, R. Y. Li, X. L. Sun, M. Cai and M. W. Verbrugge, *Advanced Functional Materials*, 2012, 22, 1647-1654.
30. S. Boukhalifa, K. Evanoff and G. Yushin, *Energy Environ. Sci.*, 2012, 5, 6872-6879.
31. X. Sun, M. Xie, J. J. Travis, G. K. Wang, H. T. Sun, J. Lian and S. M. George, *J. Phys. Chem. C*, 2013, 117, 22497-22508.
32. X. Sun, M. Xie, G. K. Wang, H. T. Sun, A. S. Cavanagh, J. J. Travis, S. M. George and J. Lian, *J. Electrochem. Soc.*, 2012, 159, A364-A369.
33. S. K. Soni, B. W. Sheldon, X. C. Xiao and A. Tokranov, *Scripta Mater.*, 2011, 64, 307-310.
34. B. J. Landi, M. J. Ganter, C. M. Schauerman, C. D. Cress and R. P. Raffaele, *J Phys Chem C*, 2008, 112, 7509-7515.
35. Y. S. Jung, A. S. Cavanagh, A. C. Dillon, M. D. Groner, S. M. George and S. H. Lee, *J Electrochem Soc*, 2010, 157, A75-A81.
36. Y. S. Jung, P. Lu, A. S. Cavanagh, C. Ban, G. H. Kim, S. H. Lee, S. M. George, S. J. Harris and A. C. Dillon, *Adv Energy Mater*, 2013, 3, 213-219.
37. Y. S. Jung, A. S. Cavanagh, L. A. Riley, S. H. Kang, A. C. Dillon, M. D. Groner, S. M. George and S. H. Lee, *Advanced Materials*, 2010, 22, 2172-+.
38. C. Li, H. P. Zhang, L. J. Fu, H. Liu, Y. P. Wu, E. Ram, R. Holze and H. Q. Wu, *Electrochim Acta*, 2006, 51, 3872-3883.
39. L. A. Riley, A. S. Cavanagh, S. M. George, S. H. Lee and A. C. Dillon, *Electrochem Solid St*, 2011, 14, A29-A31.
40. T. Hu, M. Xie, J. Zhong, H.-t. Sun, X. Sun, S. Scott, S. M. George, C.-s. Liu and J. Lian, *Carbon*, 2014, 76, 141-147.
41. N. Li, G. Liu, C. Zhen, F. Li, L. L. Zhang and H. M. Cheng, *Advanced Functional Materials*, 2011, 21, 1717-1722.
42. J. Y. Shin, D. Samuelis and J. Maier, *Adv. Funct. Mater.*, 2011, 21, 3464-3472.
43. J. H. Liu, J. S. Chen, X. F. Wei, X. W. Lou and X. W. Liu, *Adv. Mater.*, 2011, 23, 998-1002.
44. N. Li, G. Liu, C. Zhen, F. Li, L. L. Zhang and H. M. Cheng, *Adv. Funct. Mater.*, 2011, 21, 1717-1722.
45. J. Y. Shin, J. H. Joo, D. Samuelis and J. Maier, *Chem. Mater.*, 2012, 24, 543-551.
46. D. D. Cai, P. C. Lian, X. F. Zhu, S. Z. Liang, W. S. Yang and H. H. Wang, *Electrochim. Acta*, 2012, 74, 65-72.
47. S. B. Yang, X. L. Feng and K. Mullen, *Adv. Mater.*, 2011, 23, 3575-+.
48. G. K. Wang, X. Sun, F. Y. Lu, Q. K. Yu, C. S. Liu and J. Lian, *Journal of Solid State Chemistry*, 2012, 185, 172-179.
49. G. F. Ortiz, I. Hanzu, T. Djenizian, P. Lavela, J. L. Tirado and P. Knauth, *Chem. Mater.*, 2008, 21, 63-67.
50. M. Wagemaker, G. J. Kearley, A. A. van Well, H. Mutka and F. M. Mulder, *J. Am. Chem. Soc.*, 2002, 125, 840-848.
51. Y. Q. Wang, L. Guo, Y. G. Guo, H. Li, X. Q. He, S. Tsukimoto, Y. Ikuhara and L. J. Wan, *J Am Chem Soc*, 2012, 134, 7874-7879.
52. X. F. Wang, Q. Y. Xiang, B. Liu, L. J. Wang, T. Luo, D. Chen and G. Z. Shen, *Sci Rep-Uk*, 2013, 3.
53. E. M. Lotfabad, P. Kalisvaart, K. Cui, A. Kohandehghan, M. Kupsta, B. Olsen and D. Mitlin, *Phys Chem Chem Phys*, 2013, 15, 13646-13657.

54. Z. R. Zhang, Z. L. Gong and Y. Yang, *J Phys Chem B*, 2004, 108, 17546-17552.
55. S. Li, M. Ling, J. Qiu, J. Han and S. Zhang, *Journal of Materials Chemistry A*, 2015, 3, 9700-9706.
56. A. S. Cavanagh, C. A. Wilson, A. W. Weimer and S. M. George, *Nanotechnology*, 2009, 20, 255602.
57. J. A. McCormick, B. L. Cloutier, A. W. Weimer and S. M. George, *J Vac Sci Technol A*, 2007, 25, 67-74.
58. M. Ritala, M. Leskela, E. Nykanen, P. Soininen and L. Niinisto, *Thin Solid Films*, 1993, 225, 288-295.
59. M. D. Groner, J. W. Elam, F. H. Fabreguette and S. M. George, *Thin Solid Films*, 2002, 413, 186-197.
60. T. Blanquart, J. Niinisto, M. Gavagnin, V. Longo, M. Heikkila, E. Puukilainen, V. R. Pallem, C. Dussarrat, M. Ritala and M. Leskela, *Rsc Adv*, 2013, 3, 1179-1185.
61. M. Ritala, M. Leskela, E. Nykanen, P. Soininen and L. Niinisto, *Thin Solid Films*, 1993, 225, 288-295.
62. J. D. Ferguson, A. W. Weimer and S. M. George, *Chem. Mater.*, 2004, 16, 5602-5609.
63. X. Sun, M. Xie, G. K. Wang, H. T. Sun, A. S. Cavanagh, J. J. Travis, S. M. George and J. Lian, *Journal of the Electrochemical Society*, 2012, 159, A364-A369.
64. A. Pan, J.-G. Zhang, Z. Nie, G. Cao, B. W. Arey, G. Li, S.-q. Liang and J. Liu, *Journal of Materials Chemistry*, 2010, 20, 9193-9199.
65. A. Q. Pan, H. B. Wu, L. Zhang and X. W. Lou, *Energy & Environmental Science*, 2013, 6, 1476-1479.
66. D. Liu, Y. Liu, B. B. Garcia, Q. Zhang, A. Pan, Y.-H. Jeong and G. Cao, *Journal of Materials Chemistry*, 2009, 19, 8789-8795.
67. H. Liu and W. Yang, *Energy & Environmental Science*, 2011, 4, 4000-4008.
68. X. Rui, J. Zhu, W. Liu, H. Tan, D. Sim, C. Xu, H. Zhang, J. Ma, H. H. Hng, T. M. Lim and Q. Yan, *Rsc Adv*, 2011, 1, 117-122.
69. D. Yu, C. Chen, S. Xie, Y. Liu, K. Park, X. Zhou, Q. Zhang, J. Li and G. Cao, *Energy & Environmental Science*, 2011, 4, 858-861.
70. Q. Shi, R. Hu, M. Zeng, M. Dai and M. Zhu, *Electrochim Acta*, 2011, 56, 9329-9336.
71. M. Pumera, *Energy & Environmental Science*, 2011, 4, 668-674.
72. X. Sun, C. G. Zhou, M. Xie, H. T. Sun, T. Hu, F. Y. Lu, S. M. Scott, S. M. George and J. Lian, *Journal of Materials Chemistry A*, 2014, 2, 7319-7326.
73. M. Xie, X. Sun, C. Zhou, A. S. Cavanagh, H. Sun, T. Hu, G. Wang, J. Lian and S. M. George, *Journal of The Electrochemical Society*, 2015, 162, A974-A981.
74. C. M. Ban, M. Xie, X. Sun, J. J. Travis, G. K. Wang, H. T. Sun, A. C. Dillon, J. Lian and S. M. George, *Nanotechnology*, 2013, 24.
75. X. Sun, M. Xie, J. J. Travis, G. Wang, H. Sun, J. Lian and S. M. George, *The Journal of Physical Chemistry C*, 2013, 117, 22497-22508.
76. X. Sun, M. Xie, G. Wang, H. Sun, A. S. Cavanagh, J. J. Travis, S. M. George and J. Lian, *Journal of the Electrochemical Society*, 2012, 159, A364-A369.
77. P. Balaya, A. J. Bhattacharyya, J. Jamnik, Y. F. Zhukovskii, E. A. Kotomin and J. Maier, *J. Power Sources*, 2006, 159, 171-178.
78. J. Jamnik and J. Maier, *Phys. Chem. Chem. Phys.*, 2003, 5, 5215-5220.
79. J. Wang, J. Polleux, J. Lim and B. Dunn, *J. Phys. Chem. C*, 2007, 111, 14925-14931.
80. Y. F. Zhukovskii, P. Balaya, E. A. Kotomin and J. Maier, *Phys. Rev. Lett.*, 2006, 96, 058302.

Journal Name

81. B. E. Conway, *J. Electrochem. Soc.*, 1991, 138, 1539-1548.
82. M. Toupin, T. Brousse and D. Belanger, *Chem. Mater.*, 2002, 14, 3946-3952.
83. S. Boukhalifa, K. Evanoff and G. Yushin, *Energ Environ Sci*, 2012, 5, 6872-6879.
84. D. Aurbach, B. Markovsky, G. Salitra, E. Markevich, Y. Talyossef, M. Koltypin, L. Nazar, B. Ellis and D. Kovacheva, *J Power Sources*, 2007, 165, 491-499.
85. H. H. Zheng, Q. N. Sun, G. Liu, X. Y. Song and V. S. Battaglia, *J Power Sources*, 2012, 207, 134-140.
86. C. Zhan, J. Lu, A. J. Kropf, T. P. Wu, A. N. Jansen, Y. K. Sun, X. P. Qiu and K. Amine, *Nat Commun*, 2013, 4.